International Journal of Nanoelectronics and Materials
Volume 12, No. 1, Jan 2019 [55-66]

Active Control of Silver Nanostructure Aggregates for Ultrahigh Sensitive SERS Detection of Organic Molecules: Single Molecule Approach

Mehdi Q. Z[1] and Alwan M. Alwan[2]

[1,2]*Department of Applied Sciences, University of Technology, Baghdad – Iraq.*

Received 2 June 2018; Revised 10 September 2018; Accepted 21 September 2018

ABSTRACT

P-type and n-type of Porous Silicon (PSi) substrates have been prepared by electrochemical and photo-electrochemical etching processes, respectively. Unique morphological features of Psi were employed to synthesis efficient and low cost Surface-Enhanced Raman Scattering (SERS) active substances by incorporating different forms of silver nanoparticles AgNPs. Ion reduction process of silver ions by three types of PSi samples was used to develop AgNPs, Ag cluster, and Ag loop aggregates-based active SERS substrates for efficient detection of Cy3 dyes molecules. The performances of the active SERS substrates were studied extensively through analysis of scanning electron microscopy and Raman spectra. The results show that the detection process of Cy3 dyes molecules was increased with increasing the density of hot spot's regions. The developed AgNPs aggregate/p-PSi substrate with the smallest inter-particle gap size exhibits the strongest SERS enhancement and produced the best reproducibility as compared with the other two substrates. The amplified Raman efficiencies for AgNPs aggregate/p-PSi, Ag cluster aggregate/n-PSi, and Ag loop aggregate/n2-PSi substrates were calculated to be 10^{10}, 10^{6}, and 10^{3}, respectively. The experimental results show that the AgNPs aggregate/p-PSi SERS substrate exhibited significant enhancement factor of 1.07×10^{13} for 10^{-14} M dye concentration using single molecule detection technique.

Keywords: SERS, Porous Silicon, Silver Nanostructure Aggregates, Crypto Cyanine Dye.

1. INTRODUCTION

Surface-enhanced Raman Scattering (SERS) technique is widely employed to develop extremely sensitive methods for identification of molecular bio markers and small molecules [1, 2]. The main advantage of SERS is the amplification of Raman's signal at hot spot's regions as compared to Raman scattering [3]. The enhancement process of the electric field in the SERS substrate essentially depends on the density of the hot spot's regions within the nanostructured noble metal's structures [3, 4].

Among the various nanostructure noble metals, Silver Nanoparticles (AgNPs) attracted the attention of researches, as a result of excitation of Surface Plasmon Resonance (SPR) and their superior morphology properties [4, 5].

*Corresponding Author: mehdiqasim2@gmail.com

The immersion process of Porous Silicon (PSi) into the solution of $AgNO_3$ is an operant and simple method for synthesizing AgNPs through a redox process, including Ag^+ cations with the hydrides that cover the surface in the PSi layer [6-9]. The creation of pores on the silicon surface increases the coating rate, accordingly is considered a chemically active area [10, 11].

The magnitude of SERS enhancement is highly dependent on the morphology of the SERS-active substrate [12]. Thus, by tailoring morphology, and consequently, the properties of the SERS-active substrate, an extremely high sensitivity can be achieved, i.e. ultra-low concentration detection can be attained. The detection process of SERS-active substrate prepared by the immersion plating of PSi in silver salt solution strongly depended on the deposition conditions [4, 13]. The intensity of the Raman signal was found to be stronger with agglomerated forms of nanoparticles [14]. The agglomerated nanoparticles presents high density of hot spots regions [15]. Here, the performance of three types of aggregated AgNPs on PSi substrates (p-PSi, n_1-PSi and n_2-PSi) on the sensing process of Cy3 dye molecules were investigated. It is considerably worthy to carry out the detection of ultra-low concentration (single molecule regime) with simple and low-cost aggregated AgNPs /PSi substrate.

2. MATERIAL AND METHODS

2.1 Chemicals

$AgNO_3$ (99.99%), cryptocyanine Cy3 (99%), ethanol (C_2H_5OH) of 99.9% were purchased from Sigma-Aldrich Company. Hydrofluoric acid (HF) of 48% was purchased from CDH, India. The $AgNO_3$ solution was prepared by using distilled-deionized water.

2.2 PSi Sample Preparations

P-type and n-type Si (100) wafers with specific resistivity of 10 Ωcm were used to prepare PSi samples with fixed etching current density of 10 mA/cm^2 by electrochemical and photo-electrochemical etching processes, respectively. The starting Si wafers were cut into ~ 2 × 2 cm^2 pieces, cleaned in a mixture of ($HF:C_2H_5OH$=2:20) for 8 minutes and then washed with high purity ethanol. The solution of 48% HF in ethanol in the proportion of 6:4 ($HF:C_2H_5OH$) was used as the etchant. The preparation conditions of the prepared PSi samples were listed in Table 1.

Table 1 The preparation conditions of the prepared PSi samples (p-PSi, n_1-PSi and n_2-PSi).

PSi sample	Si wafer type	Etching time (min)	Illumination source
p-PSi	p-type	30	Without illumination
n_1-PSi	n-type	20	Halogen lamp (100 W/cm^2)
n_2-PSi	n-type	10	laser source with intensity of 27 mW/cm^2 and wavelength of 532 nm

2.3 SERS-Active Substrate Preparation

AgNPs were deposited on the surface of the bare etched PSi samples by immersion plating process. Bare PSi samples were immersed into the 0.01 M aqueous $AgNO_3$ solution for 10 minutes at room temperature.

The substrates for the SERS measurement were incubation for 15 seconds in solution of Cy3 which was used as an analysis in this study.

2.4 Characterizations

The morphology of the bare PSi surfaces and PSi with Ag nanoformations surfaces were studied by scanning electron microscopy (SEM) using Tescan VEGA 3 SB.

Raman spectra of the bare PSi samples and PSi with Ag nanoformations substrates were investigated using Cy3 as analyte. The bare PSi samples were soaked in a 10^{-4} M Cy3 dye solution, while PSi with Ag nanoformations substrate were soaked in a different dye concentrations of (10^{-7} M – 10^{-14} M). Raman spectra were measured with the dispersive Raman microscope (Senterra 2009, Bruker, Germany) using 785 nm of a diode laser for excitation. The spot size was ~ 2 μm, typically the ~ 50 mW laser excitation power was used and the acquisition time was 10 second.

3. RESULTS AND DISCUSSION

3.1 Morphology of PSi Samples

Three types of PSi samples (p-PSi, n_1-PSi and n_2-PSi) with different morphologies were obtained by changing the etching conditions. These samples were used as template for the SERS substrates. Figure 1(a) shows the SEM image of the p-PSi sample and it reveals that the shape of the pores is cylindrical and regular (spongiform). Figure 1(b) shows the SEM image of the n_1-PSi sample. This image exhibits that the PSi layer has cylindrical pores and trenches. Figure 1(c) shows the morphology of the n2-PSi sample and it indicates that the PSi layer has nearly uniform pores-like network.

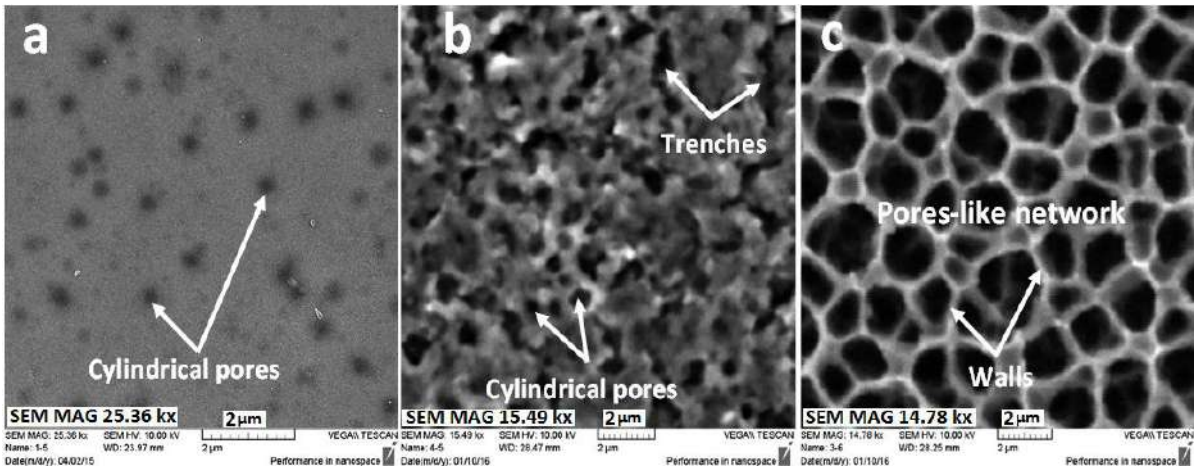

Figure 1. SEM images of three Psi samples: (a)p-Psi, (b)n_1-Psi and (c)n_2-PSi).

3.2 Morphological Features of the Silver Aggregates on the PSi Samples

Three kinds of silver aggregates formed on the surfaces of the three PSi samples (p-PSi, n_1-PSi and n_2-PSi) respectively, as clearly shown in Figure 2 which depicts the typical SEM images of these kinds of aggregates. Figure 2(a) shows the image of the AgNPs deposited on the p-PSi sample, it can be seen that the formation of AgNPs aggregates are located extremely close to each other (AgNPs aggregate/p-PSi substrate). According to a Volmer-Weber mechanism, the formation of AgNPs on the surface of p-PSi sample is due to a weak interaction between metal and the semiconductors [16,18,19]. The spongiform structure provides larger density of nucleation sites (Si-H bonds) and this makes the PSi surface more suitable for the AgNPs growth.

Figures 2(b) shows the image of another form of silver aggregates deposited on the n_1-PSi sample. It is clearly shown in this figure that the aggregates of silver clusters with sharp edges and tips are formed on the n_1-PSi sample (Ag cluster aggregate/n_1-PSi).

The last form of the silver aggregates is obtained by silver deposited on the n_2-PSi sample since AgNPs are aligned along the pores surrounding each wall to construct agglomerated silver loop (Ag loop aggregate/n_2-PSi), as they can be clearly seen in Figure 2(c).

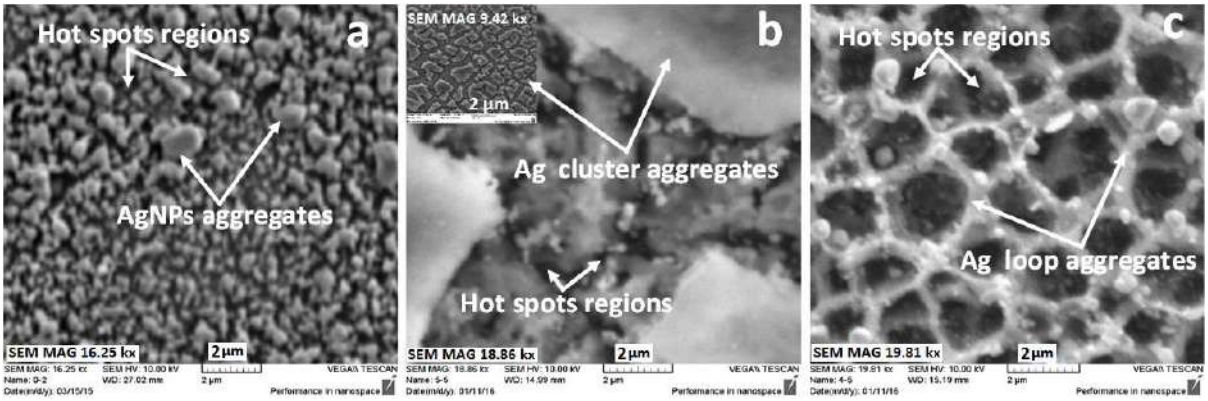

Figure 1. SEM images of the kinds of the silver aggregates at scale bar of 2 µm: (a) AgNPs aggregate ,(b) Ag cluster aggregate (the inset: view of the substrate at scale bar of 20 µm), and (c) Ag loop aggregate.

Figure 3(a), 3(b), 3(c) show the statistical distributions of the particle sizes of the three aggregates. These figures show that the sizes of the Ag particles are ranging from 3.5 to 13.5 nm for AgNPs aggregate, 7.5 to 73.5 nm for aggregate of silver clusters and 9 to 21 nm for aggregate of silver loop. The analysis of the statistical distribution of the particle sizes indicates that the sizes of the particles for all aggregates are favorable for the SERS effect.

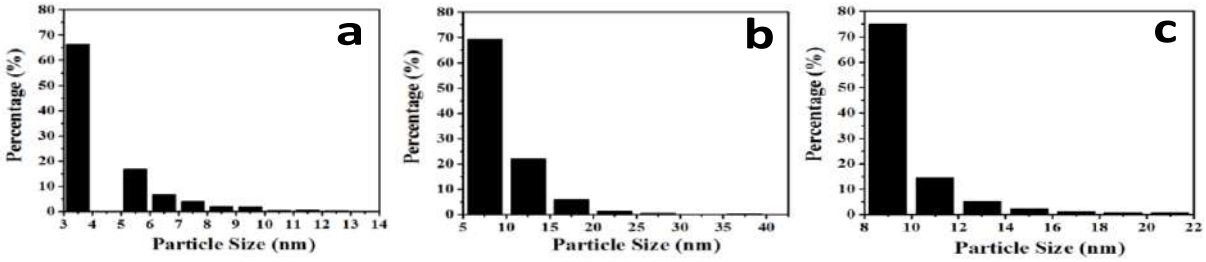

Figure 2. The statistical distribution of the particles sizes of three aggregates, (a) AgNPs aggregate, (b) silver clusters aggregate and (c) Ag loop aggregate.

Since the activity of the SERS is also affected by the distance between particles, the SERS intensity may be stronger for the tightly-packed AgNPs aggregate but not for connected AgNPs. Corresponding gap distribution histograms between particles of the three aggregates are presented in Figure 4(a), 4(b), and 4(c). The gaps of the Ag particles range from 10 to 210 nm for AgNPs aggregate, 20 to 220 nm for aggregate of silver clusters and 25 to 225 nm for aggregate of silver loop.

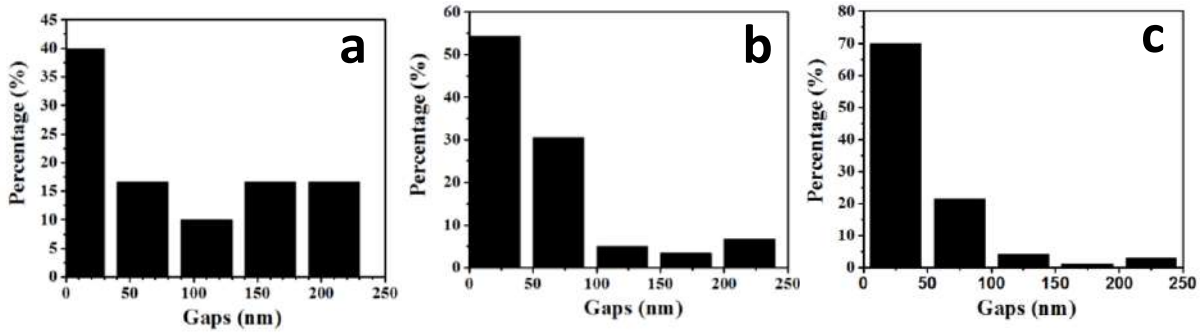

Figure 3. The statistical distribution of the gap between particles of three aggregates, (a) AgNPs aggregate, (b) silver clusters aggregate and (c) Ag loop aggregate.

3.3 Optimization of the Aggregate Kind for the SERS Activity

From Figure 5(a), 5(b) and 5(c), it is observed that the bare PSi samples show very small Raman signal with Cy3 dye for the 10^{-4} M. Whereas, the enhancement and Localized Surface Plasmon resonance (LSPR) dependency in the form of Ag aggregation is demonstrated in Figure 6. The figure reveals the SERS of low concentration which is of about 10^{-7} M Cy3 dye adsorbed on the three substrates (AgNPs aggregate/p-PSi, Ag cluster aggregate/n_1-PSi and Ag loop aggregate/n_2-PSi). It is clearly shown in this Figure 6 that the SERS enhancement was greatest for AgNPs aggregate/p-PSi substrate, which has the smallest inter-particle gap size. The SERS enhancement was weakest for Ag loop aggregate/n_2-PSi substrate, which has the largest inter-particle gap size. This behavior could be ascribed to the coupling of LSPR within two or more very close nanoparticles that yield a huge intensity of the electromagnetic field. Thus, the SERS intensity may be stronger for adsorbed molecules on substrate covered with aggregated nanoparticles. It is found that the great enhancement was attributed to only few particles (hot nanoparticles) [14]. Hence, the difference in performance of the three SERS substrates is due to the presence of hot spots which define the distance between two or more closely spaced interacting metallic particles or particles with sharp nanoscaled corners and edges where strong enhancement of the existing electromagnetic field [12]. In this experiment, suppose that aggregation has an effect on the density of the hot spots. The morphology of the AgNPs aggregate/p-PSi substrate exhibits closely-packed nanoparticles covering all the substrate surface, while the morphology of the Ag cluster aggregate/n_1-PSi shows Ag is clustered with edge. These clusters are far from each other but the morphology of the Ag loop aggregate/n_2-PSi substrate shows that the Ag aggregate surrounded the walls, i.e only walls were covered with silver but pores were not. This means that the AgNPs aggregate/p-PSi substrate has the highest hot spots density, while the Ag loop aggregate/n_2-PSi substrate has the lowest hot spots density.

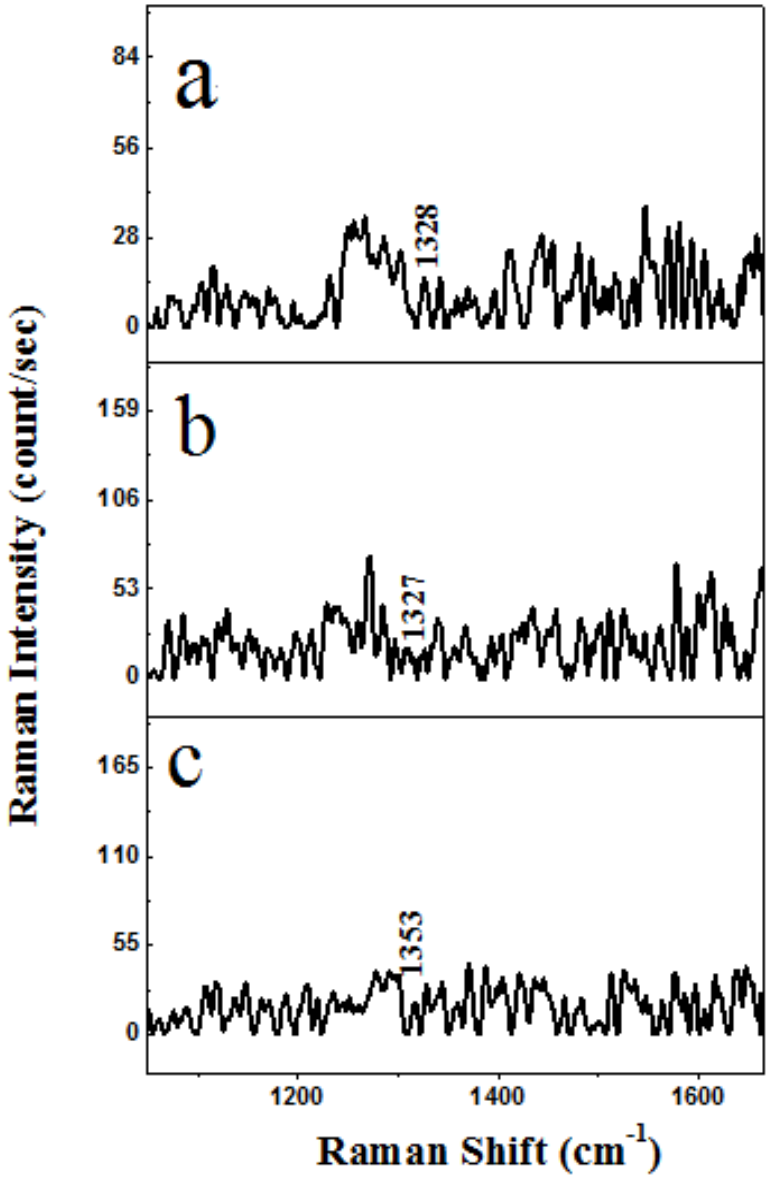

Figure 4. Raman spectra of 10^{-4}M Cy3 dye adsorped on The bare PSi samples, (a)p-PSi,(b) n_1-PSi and (c) n_2-PSi.

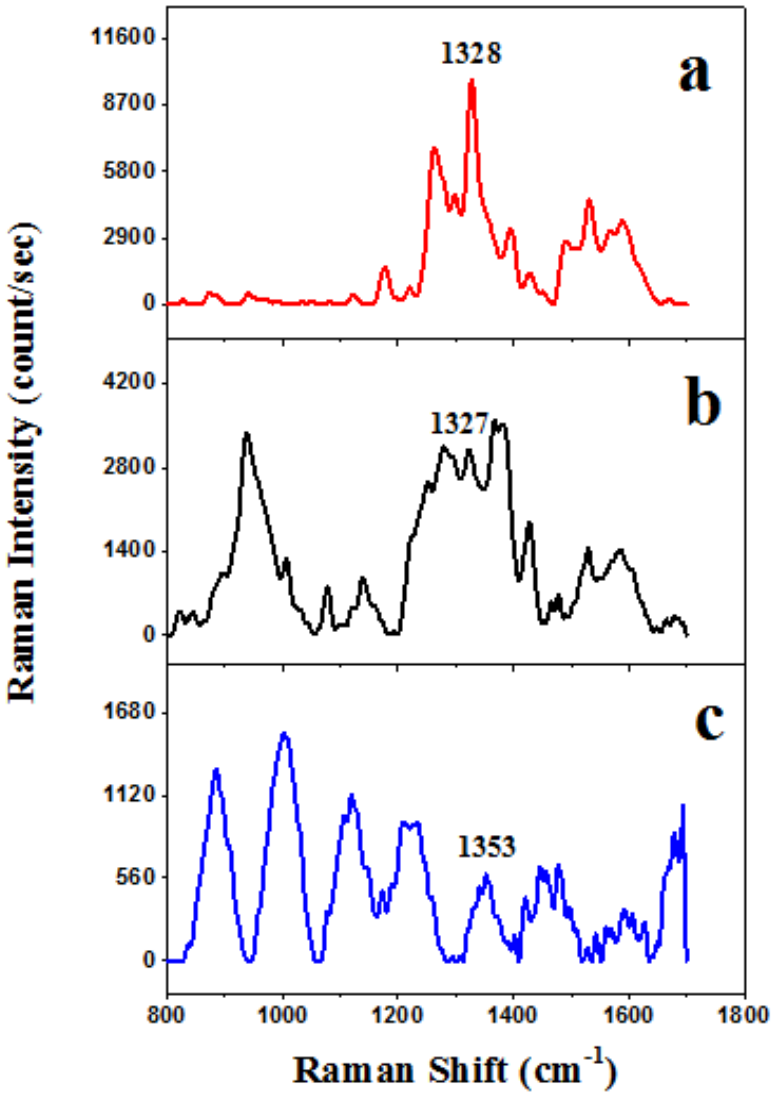

Figure 5. SERS spectra of 10^{-7}M Cy3 dye adsorped on the three substrates, (a)AgNPs aggregate/p-PSi, (b) Ag cluster aggregate/n_1-PSi and (c)Ag loop aggregate/n_2-PSi.

To estimate the reproducibility of the three substrates, a five number of random sites were selected and recording the SERS spectra was recorded. From Figure 7 which shows the reproducibility of the three substrates, it is seen that the AgNPs aggregate/p-PSi substrate exhibits the best reproducibility when compared with that of the two other substrates, while the Ag loop aggregate/n_2-PSi substrate exhibits worst reproducibility. To confirm this, the relative standard deviation of SERS intensity was calculated, and it is a 7.7%, 9.8% and 25.2% for the substrates (AgNPs aggregate/p-PSi, Ag cluster aggregate/n_1-PSi and Ag loop aggregate/n_2-PSi), respectively. This is a firm evidence of the excellent reproducibility of the AgNPs aggregate/p-PSi and Ag cluster aggregate/n_1-PSi substrates. This indicates that the reproducibility of AgNPs aggregate/p-PSi substrate is better.

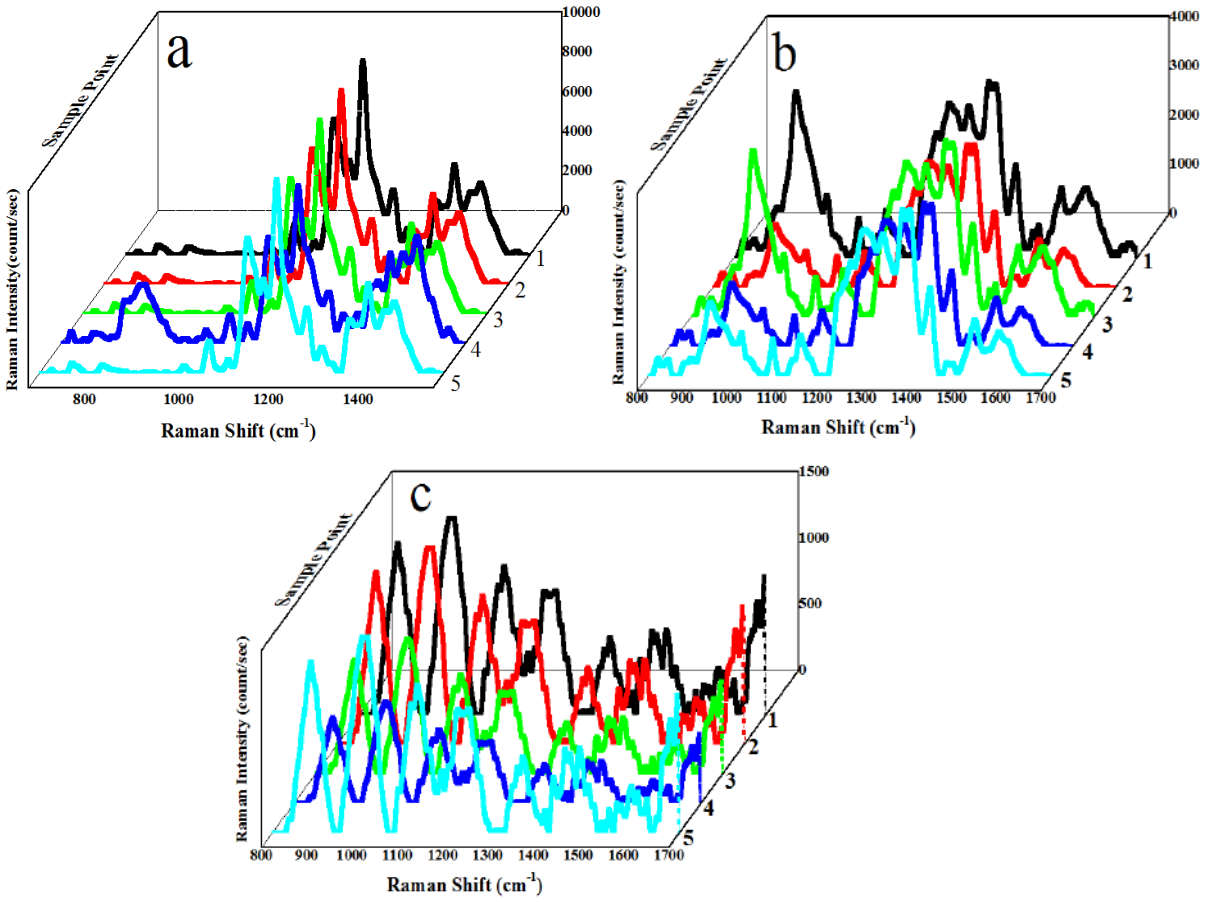

Figure 6. The reproducible SERS spectra of 10^{-7}M Cy3 dye adsorbed on (a)AgNPs aggregate/p-PSi substrate, (b) Ag cluster aggregate/n_1-PSi substrate and (c) Ag loop aggregate/n_2-PSi substrate.

At ultra-low concentration of about 10^{-14} M (single molecule approach) [4], the molecules of Cy3 dye are in homogeneously distributed throughout the substrate. Therefore, it is very likely that the single molecule detection can be obtained from a substrate that had larger number of hot spots. Thus, the concentration detection limit is a very important parameter for comparison between SERS substrates. In order to enhance the Cy3 detection limit for all SERS substrates, the Raman spectrum was measured at many random sites for each SERS substrate. Consequently, the Cy3 detection limit was estimated as shown in Figures (8 – 10). The Cy3 detection limit achieved was 10^{-14} M for AgNPs aggregate/p-PSi substrate, and 10^{-10} M for Ag cluster aggregate/n_1-PSi substrate and Ag loop aggregate/n_2-PSi substrate.

To compare between the SERS substrates, another parameter was calculated. This parameter was proposed by Virga et al. [16] and is called the External Amplified Raman Efficiency (EARE). It is defined as the ratio of minimum detectable concentration of analytic molecules obtained on bare PSi sample to the one obtained on the SERS substrate. It is found that the EAREs were 10^{10} for AgNPs aggregate/p-PSi substrate, and 10^{6} for Ag cluster aggregate/n_1-PSi substrate and 10^{3}Ag loop aggregate/n_2-PSi substrate.

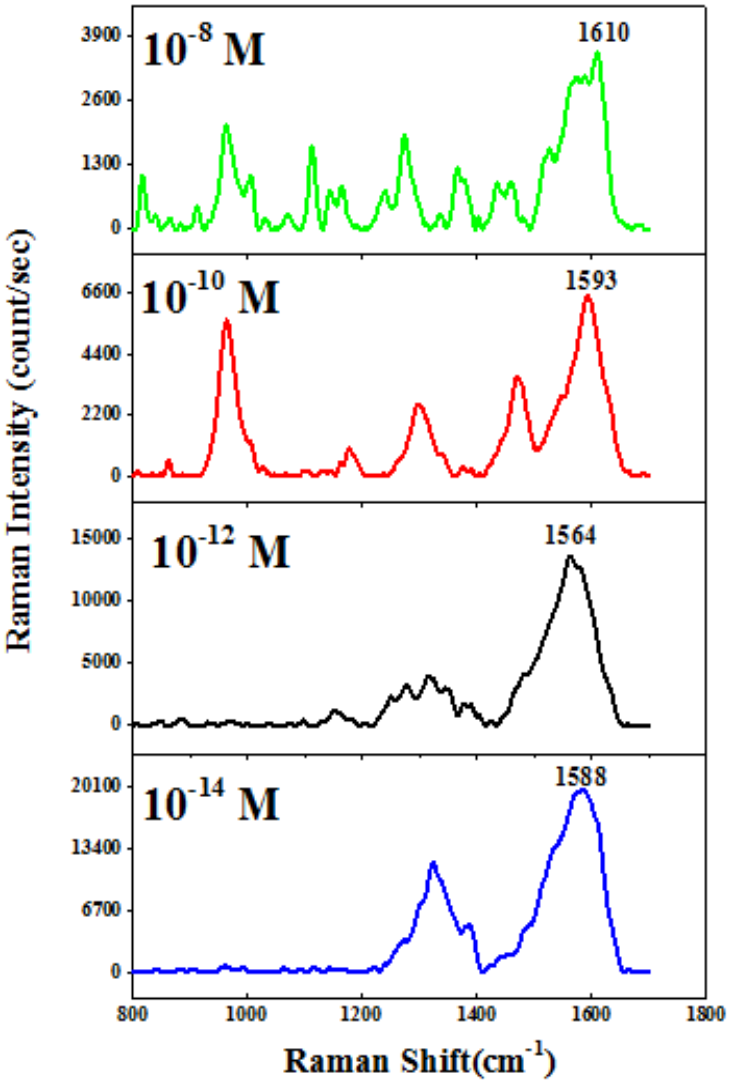

Figure 7. SERS spectra of Cy3 dye at different dye concentrations adsorped on AgNPs aggregate/p-PSi substrate.

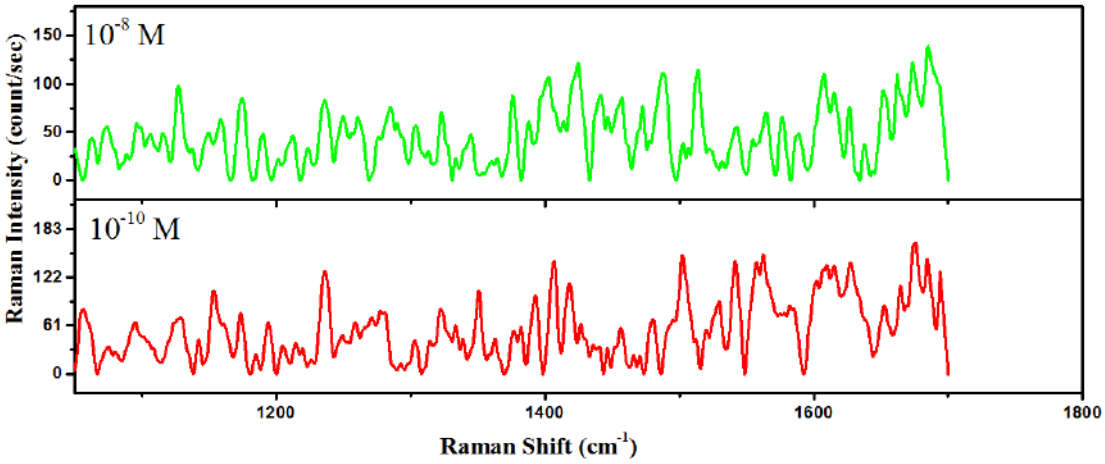

Figure 8. SERS spectra of Cy3 dye at different dye concentrations adsorped on Ag cluster aggregate/n_1-PSi substrate.

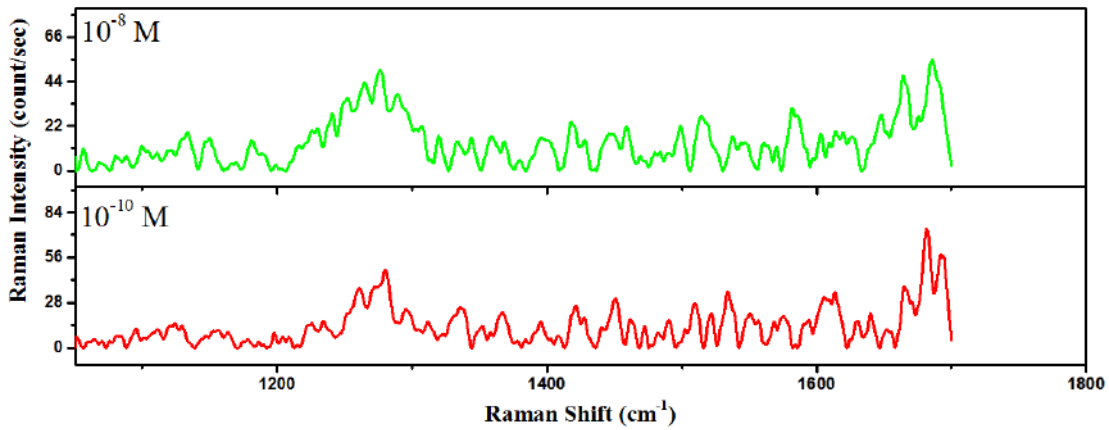

Figure 9. SERS spectra of Cy3 dye at different dye concentrations adsorped on Ag loop aggregate/n_2-PSi substrate.

Hence, the AgNPs aggregate/p-PSi substrate is very suitable for the study of the relation between Enhancement Factor (EF) and ultra-low Cy3 dye concentrations. The EF was determined using the following equation [17]:

$$EF = \frac{I_{SERS}/C_{SERS}}{I_R/C_R} \quad (1)$$

Where I_{SERS} and I_R are the intensities of the SERS and Raman, C_R and C_{SERS} are the concentrations of Cy3 for the Raman and SERS measurements, respectively.

Figure 11 shows the EF versus Cy3 concentration of Cy3 dye adsorbed on the AgNPs aggregate/p-PSi substrate. This figure indicates that the EF increases with decreasing Cy3 solution concentration. As a result, a high EF of 1.07 ×10^{13} can be obtained when using 10^{-14} M concentration.

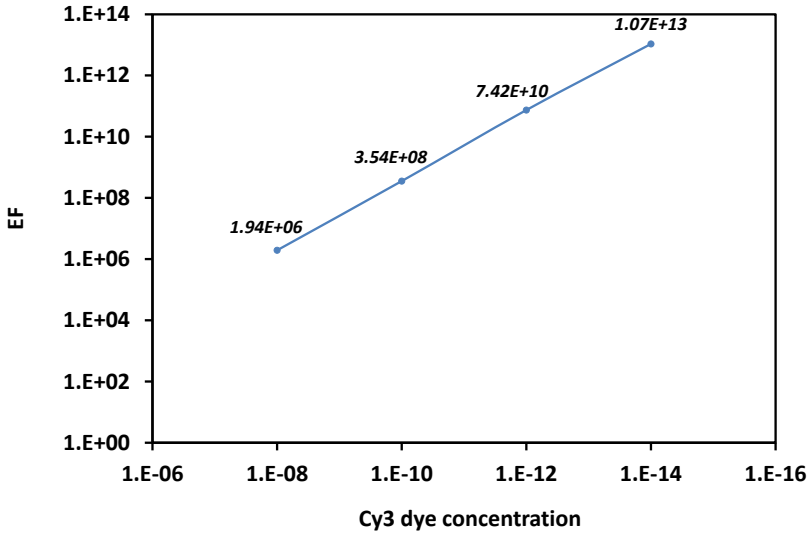

Figure 10. The EF versus Cy3 concentration of Cy3 dye adsorbed on the AgNPs aggregate/p-PSi substrate.

4. CONCLUSIONS

In this work, the effect of silver aggregate on the intensity of the SERS signal, reproducibility and detection limit were demonstrated. Controlling the silver aggregation leads to high number of hot spots obtained as to enhance the Raman's signal. The active controlling of silver aggregates was achieved by the well-controlling of the PSi morphology. The SERS activity of three kinds of Ag aggregates was estimated for ultra-low concentration of Cy3 dye. It is found that highest SERS activity with excellent reproducibility and EF of (1.07×10^{13}) is obtained when using 10^{-14} M Cy3 dyes (single molecule detection) adsorbed on the AgNPs aggregate/p-PSi substrate which has the highest number of the hot spots. The detection limit of the Ag cluster aggregate/n1-PSi and Ag loop aggregate/n_2-PSi is 10^{-10} M.

ACKNOWLEDGMENTS

I would like to express my thanks to the Department of Applied Sciences/University of Technology for assistance with samples preparation.

REFERENCES

[1] H. V. Bandarenka, K. V. Girel, V. P. Bondarenko, I. A. Khodasevich, A. Y. Panarin & S. N. Terekhov, "Formation Regularities of Plasmonic Silver Nanostructures on Porous Silicon for Effective Surface-Enhanced Raman Scattering," Nanoscale research letters **11** (2016) 1-11.

[2] N. D. Israelsen, C. Hanson & E. Vargis, "Nanoparticle properties and synthesis effects on surface-enhanced Raman scattering enhancement factor: an introduction," The Scientific World Journal **2015** (2015).

[3] A. A. Jabbar, A. M. Alwan & A. J. Haider, "Modifying and Fine Controlling of Silver Nanoparticle Nucleation Sites and SERS Performance by Double Silicon Etching Process," Plasmonics, (2017) 1-12.

[4] A. M. Alwan, A. A. Yousif & L. A. Wali, "A Study on the Morphology of the Silver Nanoparticles Deposited on the n-Type Porous Silicon Prepared Under Different Illumination Types," Plasmonics, (2017) 1-9.

[5] M. A. M. Khan, S. Kumar, M. Ahamed, S. A. Alrokayan & M. S. AlSalhi, "Structural and thermal studies of silver nanoparticles and electrical transport study of their thin films," Nanoscale research letters **6** (2011) 434.

[6] F. Giorgis, E. Descrovi, A. Chiodoni, E. Froner, M. Scarpa, A. Venturello, *et al.,* "Porous silicon as efficient surface enhanced Raman scattering (SERS) substrate," Applied Surface Science **254** (2008) 7494-7497.

[7] A. Y. Panarin, S. Terekhov, K. Kholostov & V. Bondarenko, "SERS-active substrates based on n-type porous silicon," Applied Surface Science **256** (2010) 6969-6976.

[8] E. Nativ-Roth, K. Rechav & Z. e. Porat, "Deposition of gold and silver on porous silicon and inside the pores," Thin Solid Films **603** (2016) 88-96.

[9] A. M. Alwan, A. J. Hayder & A. A. Jabbar, "Study on morphological and structural properties of silver plating on laser etched silicon," Surface and Coatings Technology **283** (2015) 22-28.

[10] F. Harraz, T. Tsuboi, J. Sasano, T. Sakka & Y. Ogata, "Metal deposition onto a porous silicon layer by immersion plating from aqueous and nonaqueous solutions," Journal of The Electrochemical Society **149** (2002) C456-C463.

[11] A. M. Alwan & A. B. Dheyab, "Room temperature CO2 gas sensors of AuNPs/mesoPSi hybrid structures," Applied Nanoscience **7** (2017) 335-341.

[12] M. Kosović, M. Balarin, M. Ivanda, V. Đerek, M. Marciuš, M. Ristić, *et al.,* "Porous silicon covered with silver nanoparticles as surface-enhanced Raman scattering (SERS) substrate for ultra-low concentration detection," Applied spectroscopy **69** (2015) 1417-1424.
[13] J. H. Adawyia, M. A. Alwan & A. J. Allaa, "Optimizing of porous silicon morphology for synthesis of silver nanoparticles," Microporous and Mesoporous Materials **227** (2016) 152-160.
[14] G. Wei, H. Zhou, Z. Liu & Z. Li, "A simple method for the preparation of ultrahigh sensitivity surface enhanced Raman scattering (SERS) active substrate," Applied Surface Science **240**, (2005) 260-267.
[15] A. F. Chrimes, K. Khoshmanesh, P. R. Stoddart, A. A. Kayani, A. Mitchell, H. Daima, *et al.,* "Active control of silver nanoparticles spacing using dielectrophoresis for surface-enhanced Raman scattering," Analytical chemistry **84** (2012) 4029-4035.
[16] A. Virga, P. Rivolo, E. Descrovi, A. Chiolerio, G. Digregorio, F. Frascella, *et al.,* "SERS active Ag nanoparticles in mesoporous silicon: detection of organic molecules and peptide–antibody assays," Journal of Raman Spectroscopy **43** (2012) 730-736.
[17] R. Botta, G. Upender, R. Sathyavathi, D. N. Rao & C. Bansal, "Silver nanoclusters films for single molecule detection using Surface Enhanced Raman Scattering (SERS)," Materials chemistry and Physics **137** (2013) 699-703.
[18] Alwan M. Alwan, Duaa A. Hashim & Muslim F. Jawad "Optimizing of porous silicon alloying process with bimetallic nanoparticles" Springer Nature Switzerland AG, 19 May 2018 /Accepted: 14 July 2018.
[19] Layla A. Wali, Khulood K. Hasan & Alwan M. Alwan "Rapid and Highly Efficient Detection of Ultra-low Concentration of Penicillin G by Gold Nanoparticles/Porous Silicon SERS Active Substrate" Spectrochimica Acta Part A: Molecular and Biomolecular Spectroscopy **206** (2019) 31.